Solvent-enhanced dye diffusion in polymer thin films for polymer light-emitting diode application

Troy Graves-Abe,[a] Florian Pschenitzka,[b] H. Z. Jin, Brent Bollman,[c] and J. C. Sturm
Department of Electrical Engineering, Princeton Institute for the Science and Technology of Materials, Princeton University, Princeton, New Jersey 08544

R. A. Register
Department of Chemical Engineering, Princeton Institute for the Science and Technology of Materials, Princeton University, Princeton, New Jersey 08544

(Received 21 May 2004; accepted 24 August 2004)

The method of solvent-enhanced dye diffusion for patterning full-color (red, green, and blue) polymer light-emitting diode displays was investigated in detail. After local dry transfer of dye onto a device polymer film, the dye remains on the surface of the polymer layer and must be diffused into the polymer for efficient emission. Exposure of the polymer to solvent vapor at room temperature increases the dye-diffusion coefficient by many orders of magnitude, allowing rapid diffusion of the dye into the film without a long, high-temperature anneal that can degrade the polymer. The increase in diffusion is due to absorption of the solvent vapor into the polymer film, which increases the polymer thickness and decreases its effective glass transition temperature $T_{g,\mathrm{eff}}$. Measurements of the polymer in solvent vapor indicate that its thickness varies roughly linearly with pressure and inversely with temperature, with thickness increases as large as 15% often observed. A model based on Flory-Huggins theory is used to describe these results. The diffusion of the dye into the polymer was evaluated by photoluminescence and secondary-ion mass spectroscopy. This dye-diffusion increase is largest for high solvent-vapor partial pressures and, most surprisingly, is larger at lower temperatures than at higher temperatures. This anomalous temperature dependence is due to the increased solvent-vapor absorption and consequent reduction in the effective glass-transition temperature at lower temperatures. © *2004 American Institute of Physics*.
[DOI: 10.1063/1.1806548]

I. INTRODUCTION

Polymer light-emitting diodes (PLEDs) have emerged as a very promising candidate for commercial displays, and first-generation PLED displays can already be found in the marketplace.[1] PLEDs are appealing in part because the polymer layer can be deposited by a low-cost spin-coating process. In most cases, further patterning is then necessary if the polymer is to be used in a full-color display, because the as-deposited uniform film is generally limited to emission of only one color.

Several groups have suggested the use of a dry dye transfer from a large-area dye source to pattern the local emission color of the polymer film as a route toward the integration of red, green, and blue (RGB) PLEDs.[2–5] These dry transfer processes are attractive compared to inkjet printing of the dye because they can in principle cover large areas in one step and because they avoid film uniformity and lateral redistribution problems which occur during the drying of the printed droplets.[6–9] In dry printing, the dye can be thermally transferred to the emissive polymer by printing from a prepatterned polymer stamp containing the dye [Fig. 1(a)].[10] However, the transferred dye tends to accumulate on the surface of the polymer film, where it is mostly inactive due to the lack of energy transfer from the host polymer, or inefficient due to dye concentration quenching [Fig. 1(b)]. Treating the sample in solvent vapor after the initial dye transfer was found to promote the rapid diffusion of the transferred dye throughout the thickness of the polymer at room temperature [Figs. 1(c) and 1(d)]. This redistribution process otherwise required annealing at temperatures near the polymer glass transition temperature (T_g), where the polymer could degrade.

In this paper, the process of solvent-enhanced dye diffusion in polymers for PLEDs is investigated in detail. In Sec. II, an overview of the process and past work is given. Section III A presents experimental results for the increase in thickness of the device polymer as a function of solvent, vapor-exposure time, vapor pressure, and temperature, and Sec. III B presents a model for these effects. Finally, Sec. IV A describes experimental results for actual dye diffusion in the presence of solvent vapor, and Sec. IV B describes the increase in dye diffusion as due to the free volume increase caused by the solvent. A separate paper will focus on the technology development associated with the approach, including patterning of the stamp, device and process optimization, and the integration of red, green, and blue PLEDs.[11]

[a]Electronic mail: tabe@princeton.edu
[b]Present address: OSRAM Opto Semiconductors, Inc., 3870 North First Street, San Jose, CA 95134.
[c]Present address: Nanosolar, 2440 Embarcadero Way, Palo Alto, CA 94303.

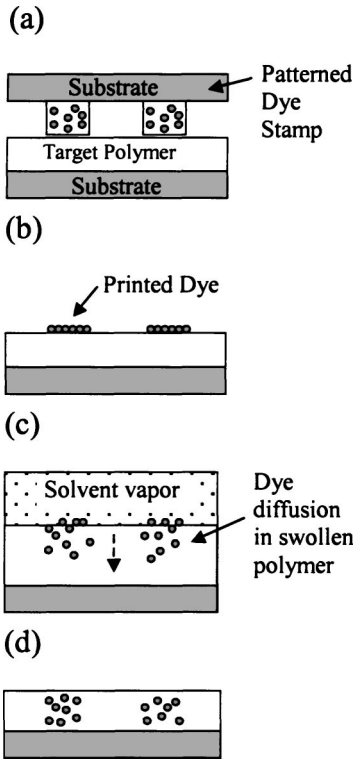

FIG. 1. Schematic overview of patterned dye printing and subsequent dye diffusion. (a) Dye is printed onto target device polymer from prepatterned polymer containing dye. (b) Printed dye remains at or near the surface of the dye. (c) Polymer is exposed to solvent vapor and swells; dye diffuses rapidly into the film. (d) Polymer returns to its original thickness after the solvent vapor is removed. Vertical dimensions are exaggerated vs lateral dimensions.

II. BACKGROUND ON SOLVENT-ENHANCED DYE DIFFUSION IN POLYMERS

A. Dye transfer

Spin coating or blade coating of the emissive polymer in PLED displays is desirable because both are simple and low cost. A patterning process must then generally be used to locally introduce dye into the polymer film to obtain a full-color, RGB display (alternatively, there have also been reports of selectively deactivating globally distributed dyes through patterned UV radiation[12]). Initial work to locally introduce a dye utilized a shadow mask placed between the dye source and the target polymer layer.[2] However, this approach resulted in damage to the polymer layer due to physical contact between the metal mask and soft polymer. An alternative soft printing process was therefore developed.[13] In this procedure, a "stamp" is prepared by spin-coating the polymer Vylon 103 (obtained from Toyoba, M_w $\sim$20 000–25 000 g/mol, 98% by weight) doped with a dye, in this case coumarin-6 (C6, emission peak at 495 nm, 2% by weight), onto a glass substrate. The device polymer consists of a thin (80–120 nm) film of the hole-transport polymer poly(9-vinlycarbazole) (PVK) (M_w ca. 1 100 000 g/mol, 71% by weight in the final film) mixed with the electron-transport molecule 2-(4-Biphenylyl)-5-(4-tert-butyl-phenyl)-1,3,4-oxadiazole (PBD) (29% by weight) deposited by spin-coating from solution (100 mg PVK, 40 mg PBD, and 7.5 mL chlorobenzene) onto an indium-tin oxide (ITO)-coated glass substrate.[14] After patterning the stamp, the dye is printed onto the top of the device polymer by placing the target and source films in direct contact in vacuum at elevated temperatures (60 °C–80 °C) for 20–60 min.

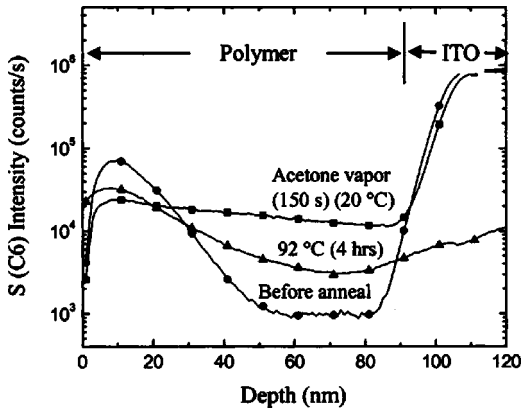

FIG. 2. SIMS profiles of sulfur (from C6 dye) in a 90-nm PVK/PBD film with printed C6 layer before annealing (circles), after a 4-h anneal at 92 °C in vacuum (triangles) and a 150-s anneal at 20 °C in acetone vapor (90 torr) (squares). The rise of all signals after 80 nm is a SIMS artifact.

Following printing, the dye is concentrated at the polymer surface, where its photoluminescence (PL) efficiency is limited by a lack of energy transfer from the polymer and/or dye concentration quenching. Secondary-ion-mass spectroscopy (SIMS) was used to measure the initial dye distribution.[15] Because only the C6 contains sulfur, the sulfur signal is used to mark the position of the C6 in the polymer film. Prior to annealing, the sulfur signal from the as-printed sample shows a peak near the surface of the sample and extends 40 nm into the sample, dropping to negligible levels between 40 and 80 nm and then rising rapidly after 80 nm (Fig. 2). Both the exponentially decaying tail of the profile into the sample and the rise of the signal at 80 nm are SIMS artifacts. The rise at 80 nm is from an $^{16}O_2^+$ signal (oxygen from the ITO) being misinterpreted as $^{32}S^+$. Spurious signals within the polymer could also arise if the sample was not sufficiently outgassed in the SIMS chamber to remove O_2 (or water) that had been absorbed by the polymer prior to loading. The exponentially decaying tail near the surface does not represent any initial diffusion of the dye into the film during the printing step and is instead due to well-known "knock-on" effects. These effects occur when the Cs^+ primary ion (for sputtering the surface) displaces the lighter sulfur atoms toward deeper locations during the measurement. This was confirmed by a control sample consisting of a thin layer of C6 that was evaporated directly onto the PVK/PBD layer (without heating); SIMS measurements on this sample revealed a similar profile to the printed dye. The 70-°C printing step is therefore not adequate to diffuse the dye into the polymer and instead leaves the C6 accumulated on its surface.

B. Dye diffusion

The dye can be diffused into the polymer by annealing in vacuum at elevated temperatures for long time periods. Figure 2 shows that after 4 h at 92 °C, the C6 has diffused but

is still far from uniformly dispersed. Annealing at higher temperatures is not practical as the glass transition temperature T_g for this blend is only 120 °C.[16] Furthermore, the use of a polymer with a lower T_g is not a viable approach because device polymers with a high T_g are desired for PLED reliability.

A process to temporarily enhance the dye diffusion without later compromising the device performance was therefore developed. Following dye printing, the polymer is exposed to solvent vapor, which it absorbs. The absorption of the solvent vapor causes an increase in the polymer's free volume. The increase in free volume dramatically enhances the diffusion of the dye into the film, allowing the diffusion to take place at a low temperature (e.g., room temperature) without damage to the polymer film. Finally, the polymer is dried in nitrogen, causing it to return to its original thickness and slow-diffusion condition.

Only 150 s in acetone vapor (partial pressure = 90 torr) at room temperature is necessary to ensure that the printed C6 is distributed nearly uniformly throughout the PVK/PBD (Fig. 2). Thus the 150-s room-temperature treatment in acetone vapor causes a far larger amount of diffusion than the 4-h anneal at 92 °C, demonstrating that the solvent vapor causes a remarkable increase in the diffusion coefficient of the dye. The next two sections seek to fundamentally understand and characterize this enhanced diffusion.

III. POLYMER THICKNESS AND INDEX OF REFRACTION CHANGES UNDER SOLVENT-VAPOR EXPOSURE

A. Measurement of changes in polymer thickness and index of refraction

Because it was expected that the enhancement of dye diffusion in solvent vapor would depend on the amount of solvent imbibed by the film, we investigated in detail the thickness increase of PVK/PBD films upon exposure to solvent vapor under various conditions. In this section, we present experimental results (Sec. III A) and a model (Sec. III B) for the dependence of PVK/PBD thickness and index of refraction on choice of solvent, solvent vapor pressure, and sample temperature.

A Filmetrics F20 reflectance spectrometer was used for *in situ* monitoring of polymer thickness and optical constants under solvent vapor exposure. For such measurements, PVK/PBD films of varying thickness were deposited by spin-coating onto silicon substrates. The normal-incidence reflectance spectrum from a tungsten-halogen bulb was recorded over a range of 450–850 nm, where the absorption in PVK is negligible.[17] By measuring the bare silicon reflectance and assuming the polymer extinction coefficient in the wavelength range is zero, it is straightforward to extract the film thickness t_f and index of refraction n_f by fitting the measured reflectance profile to that expected from a simple interference model.[18] For this, we assumed the three-parameter Cauchy model for the wavelength dependence of n_f:

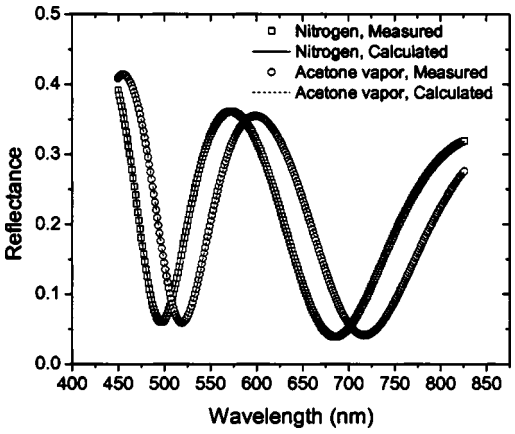

FIG. 3. Measured and fitted reflectance spectra of a PVK/PBD film on silicon in nitrogen (squares) and in acetone vapor (120 torr, 20 °C) (circles). The best 4-parameter fit to the reflectance spectrum in nitrogen corresponds to $t_f = 536$ nm, $A = 1.58$, $B = 6980$ nm^2, and $C = 8.05 \times 10^8$ nm^4, and in acetone vapor, $t_f = 567$ nm, $A = 1.56$, $B = 7140$ nm^2, and $C = 8.14 \times 10^8$ nm^4.

$$n_f(\lambda) = A + \frac{B}{\lambda^2} + \frac{C}{\lambda^4}. \tag{1}$$

The three parameters A, B, and C, along with t_f, were used as four adjustable parameters to fit the reflectance spectrum (Fig. 3). Some caution was necessary for thin films (<80 nm for PVK/PBD), in which the number of extrema in the reflectance spectrum was not sufficient for a unique determination of all the parameters. In these cases, A, B, and C, calculated from measurements of thicker PVK/PBD layers under similar conditions were used to ensure an accurate determination of t_f. Upon exposure of the film to solvent vapor, the film absorbs the vapor, causing an increase in t_f and decrease in n_f that can be measured by the change in the reflectance spectrum (Fig. 3). Exposure of a bare silicon wafer to solvent vapor caused no change in the reflectance, so all the changes under solvent vapor were due to changes in the polymer.

Measurements of the increase of PVK/PBD thickness at saturated vapor pressure for several different solvents were taken in small-volume chambers (60–1000 cm^3) by placing a small quantity of the solvent in the nearly closed chamber and allowing the solvent to partially evaporate over a long period of time (10–40 min) at room temperature. The thickness increases are plotted versus the solvents' Hildebrand solubility parameters in Fig. 4. Hildebrand solubility parameters are derived from the square root of the cohesive energy density of the solvent and provide a simple estimate of their relative solvency behaviors.[19] The trend depicted in Fig. 4 resembles the observed solvency behavior of PVK, with the saturated vapor of chloroform (which readily dissolves PVK) yielding the highest thickness increase of 48%. The rest of the measured solvents do not dissolve PVK and correspondingly have lower thickness increases that decrease in magnitude for solubility parameters that are increasingly dissimilar to that of chloroform. Because PVK is soluble in chloroform, the film thickness in saturated chloroform vapor should theoretically increase without limit as chloroform condenses into solution in the film. Although some instability in the thickness of the film in chloroform vapor was observed, the thick-

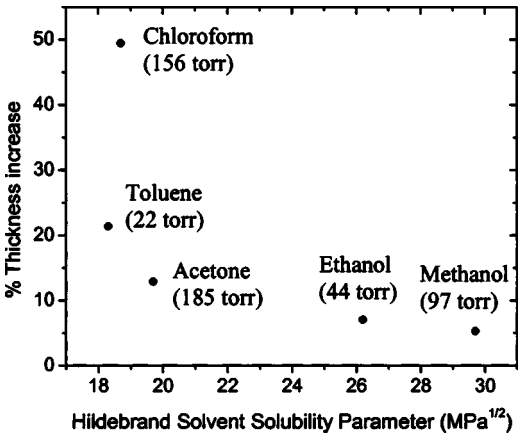

FIG. 4. PVK/PBD thickness increase in various solvents at saturated vapor pressures at 20 °C.

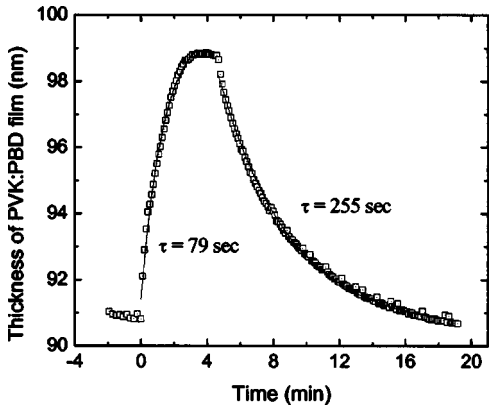

FIG. 6. Time dependence of PVK/PBD swelling upon exposure to acetone vapor (120 torr) in nitrogen at 0 min, followed by drying in a pure nitrogen after the acetone vapor was turned off at 5 min.

ness remained finite, suggesting that the actual chloroform partial pressure may have remained slightly below the saturation pressure. The instability of the PVK/PBD thickness in chloroform due to its strong solvency behavior led us to choose acetone, which does not dissolve PVK but still had a relatively large thickness increase, as a candidate for more detailed study.

For measurements at different acetone partial pressures and sample temperatures, PVK/PBD films were placed in a chamber consisting of a temperature-controlled sample stage mounted in a glass cylinder connected to a gas supply and exhaust (Fig. 5). The partial pressure of the solvent vapor in the gas supply was varied by mixing pure nitrogen with nitrogen bubbled through a wash bottle containing liquid solvent. This wash bottle was kept in a water bath to maintain a constant temperature as the solvent evaporated. Partial pressures were calculated by measuring the amount of liquid solvent evaporated and the nitrogen flow rate.

Figure 6 shows how the thickness of a PVK/PBD film changes upon exposure to solvent vapor at room temperature. Initially, a thickness of 91 nm was measured in a flow of dry nitrogen. Acetone vapor (~120 torr) was then added to the nitrogen and the thickness of the film rapidly increased to 99 nm. After 5 min, the acetone vapor was removed and the film returned to its original thickness as it was dried by the flow of pure nitrogen. Fitting the increase and decrease of the thickness versus time with an exponential function yields time constants of 79 and 255 s, respectively. A rough estimate of the time constant is determined by dividing the chamber volume (8.6 L) by the gas flow rate (~4 L/min for each case) to obtain 130 s, which shows that a large part of the time constants are simply due to gas residence times and not to delays in the uptake of the solvent. The discrepancy between the experimental time constants for increasing and decreasing thickness (79 and 255 s) and the estimated time constant (130 s) is not understood and may be related to the actual absorption/desorption mechanisms. That much of the time constants are due to the gas dynamics was further confirmed by an experiment using a much smaller (34 cm^3) volume where only the thickness-increase time constant was measured. Using this smaller volume, a time constant of 1 s was observed, confirming that gas mixing in the larger chamber dominates the measured time constants.

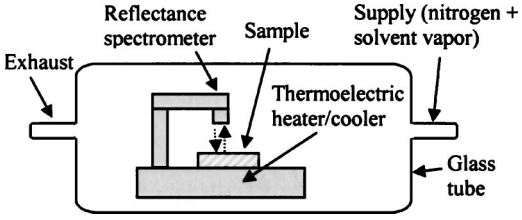

FIG. 5. Schematic of experimental apparatus used for dye diffusion at different sample temperatures and solvent-vapor partial pressures. A Filmetrics F20 reflectance spectrometer was used for the *in situ* measurement of the polymer thickness.

Further measurements of film thickness increases under various conditions were taken by waiting for 5 min after solvent vapor exposure to ensure that the film had reached equilibrium. At room temperature (19 °C), the equilibrium increase in the PVK/PBD thickness was roughly linear with respect to acetone partial pressure up to 130 torr, where its thickness increase was 8% [Fig. 7(a)]. Similar trends were observed at higher (45 °C) and lower (10 °C) temperatures. Interestingly, the thickness increase in the PVK/PBD film becomes larger at lower sample temperatures (for a constant acetone-vapor pressure), and a roughly inverse dependence on temperature was measured [Fig. 7(b)]. Qualitatively, this inverse temperature dependence is due to the solvent's tendency to evaporate from the PVK/PBD film at elevated temperatures, where its saturation vapor pressure is higher. Over the pressure and temperature range shown in Fig. 7, the polymer could be returned to its original thickness by removing the acetone vapor and drying it with nitrogen.

As the polymer film absorbed acetone vapor, its index of refraction decreased. This decrease was roughly uniform over the 450–850 nm range that we studied and is shown in Fig. 8 for an acetone-vapor pressure of 120 torr at 19 °C, corresponding to a film thickness increase of 7%. A decrease in the index of refraction is expected as acetone (with a low n) is absorbed into the higher-n film and is modeled in the next section.

We should note that despite considerable effort, we observed that the measured thickness change could vary significantly (up to even a factor of 2) when similar experiments

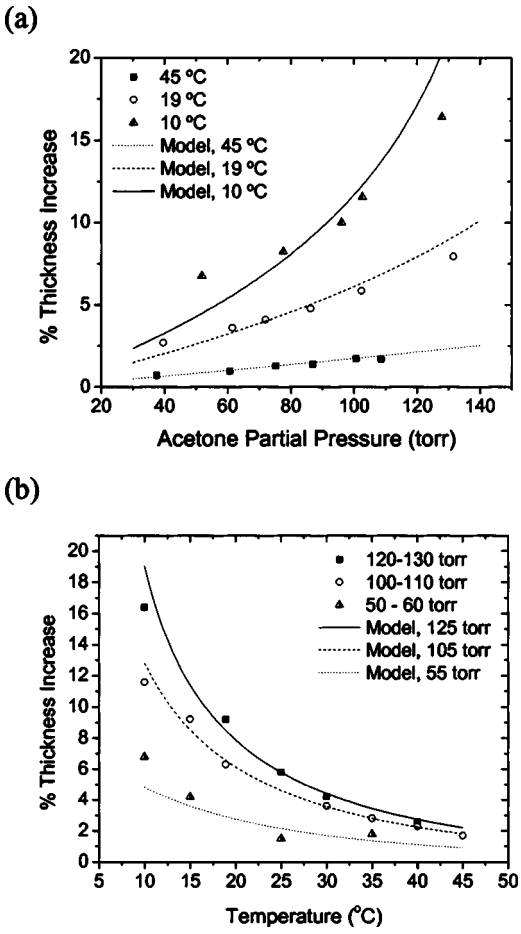

FIG. 7. (a) Experimental and modeled PVK/PBD thickness increases plotted vs acetone partial pressure for several different sample temperatures. (b) Experimental and modeled PVK/PBD thickness increases plotted vs sample temperature for different acetone partial pressures. Due to the difficulty in maintaining a constant partial pressure, each experimental partial pressure corresponds to a range of 10 torr. Dry film thickness ranged from 80 to 100 nm. The model contains one adjustable fitting parameter: the Flory-Huggins interaction parameter χ, set equal to 1.53 for all the calculations shown.

were conducted months apart. This variation may be due to changes in the temperature calibration, adjustments in the experimental apparatus, variations in the acetone temperature (and evaporation rate), leaks in the chamber apparatus, or perhaps heating from the absorption of the white-light source used in the reflectometry measurements. The problem was especially severe for acetone partial pressures near the saturated vapor pressure and low temperatures (<10 °C), which led to large solvent absorption and thickness increases (up to 30%). In some cases near the saturated vapor pressure, large and irreversible increases in film thickness were measured, along with significant roughening of the polymer layer. Micrographs of the roughened polymer layers indicated that some crystallization of the PBD had occurred (the PVK is atactic and cannot crystallize). The possibility of PBD crystallization led us to generally restrict measurements to film thickness increases below 15%. To examine the possibility of other changes in the microstructure of the PVK/PBD film caused by lesser solvent-vapor exposures, cathodes (10:1 Mg:Ag to a thickness of 50 nm, followed by 50 nm of Ag) were deposited by thermal evaporation onto PVK/PBD devices (with C6 present in the spun-on film) after exposing the PVK/PBD/C6 layer to acetone vapor (120 torr for 10 min at 19 °C, corresponding to a thickness increase of ~10%). The forward-bias and electroluminescent characteristics of devices exposed to acetone vapor remained similar to control devices fabricated without vapor exposure. Because the current-voltage and electroluminescent characteristics of these devices are intimately dependent on the microstructure of the organic layer, this suggests that no significant changes in the PVK/PBD microstructure take place during absorption of solvent vapor for thickness increases below ~15%.

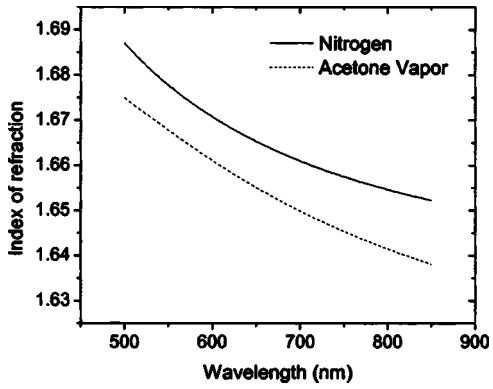

FIG. 8. Index of refraction vs wavelength for PVK/PBD in a pure nitrogen (solid line) and during exposure to acetone vapor (120 torr) (dashed line) at 19 °C (thickness increase of 7%, from 89 to 95 nm). The addition of acetone with a lower n decreases n_f of the film.

B. Modeling of the change in polymer index of refraction and film thickness due to solvent vapor

The decrease in index of refraction of the PVK/PBD films upon exposure to acetone vapor (as measured by reflectance spectroscopy and parameter fitting) was modeled by using the Lorentz-Lorenz relationship.[20] In this approximation, the effective index of refraction of the binary mixture (n_f) is related to the indices of refraction n_s and n_p of the solvent and polymer, and the volume fraction ϕ_s of the solvent

$$\frac{n_f^2-1}{n_f^2+2}=\phi_s\frac{n_s^2-1}{n_s^2+2}+(1-\phi_s)\frac{n_p^2-1}{n_p^2+2}. \tag{2}$$

The polymer index of refraction n_p for the PVK/PBD blend (with no solvent) was measured to be 1.677 (at $\lambda=589$ nm, corresponding to the D line of sodium), and for n_s the index of refraction of liquid acetone of 1.36 (at 589 nm) was used. The volume fraction ϕ_s of acetone can be estimated by assuming that it is equal to the measured thickness increase of the PVK/PBD film:

$$\phi_s=\frac{t_{\mathrm{solv}}-t_{\mathrm{dry}}}{t_{\mathrm{solv}}}, \tag{3}$$

where t_{solv} is the thickness in solvent vapor and t_{dry} is the original thickness. With these values, the calculated n_f from Eq. (2) agrees very well with n_f obtained by reflectometry over a range of polymer film thickness increases with no adjustable parameters (Fig. 9). The correspondence between model and data indicates that our assumption that the extra

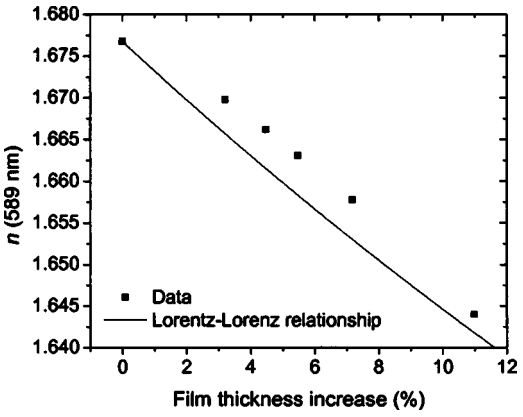

FIG. 9. Measured index of refraction (at $\lambda = 589$ nm) for a PVK/PBD film (dry thickness of 100 nm) vs the film thickness change at 17 °C in acetone vapor (partial pressures up to 130 torr) (squares). Also shown is the index of refraction calculated from the Lorentz-Lorenz relationship by using the measured increase in film thickness (with no adjustable parameters) (solid line).

volume of the film is equal to that occupied by acetone at its liquid density is reasonable. Furthermore, it gives us confidence that the reflectance spectroscopy and parameter-fitting procedure is yielding correct information on film thickness and index of refraction.

A model was developed to express the PVK/PBD thickness increase as a function of solvent partial pressure and sample temperature. In this model, we first approximate the mixture of high-molecular-weight PVK and small-molecule PBD as a uniform, high-molecular-weight polymer. Flory-Huggins theory[21] can then be used to describe the excess Gibbs free energy (G^E) of the polymer-solvent mixture:

$$G^E/RT = \left[x_s \ln\left(\frac{\phi_s}{x_s}\right) + x_p \ln\left(\frac{\phi_p}{x_p}\right) \right] + \chi(x_s + m x_p)\phi_s\phi_p. \tag{4}$$

Here, ϕ_p is the polymer volume, x_s and x_p are the mole fractions of the solvent and polymer in the mixture, R is the ideal gas constant, T is the temperature, and m is the ratio of the polymer molar volume to the solvent molar volume. The Flory-Huggins polymer-solvent interaction parameter, χ, is a parameter that represents the strength of the solvent-polymer interaction. Equation (4) can be used to derive an expression for the solvent activity coefficient (γ_s) from the relation[22]

$$\ln(\gamma_s) = \left[\frac{\partial\left(\frac{nG^E}{RT}\right)}{\partial n_s} \right]_{p,T,n_p}. \tag{5}$$

Here, n is the total number of molecules in the mixture so that $n_s = x_s n$. Evaluation of Eq. (5) leads to

$$\ln(\gamma_s) = \ln(\phi_s/x_s) + (1 - m^{-1})\phi_p + \chi(\phi_p)^2. \tag{6}$$

Next, we assume that an equilibrium exists between the composition of the solvent-swollen polymer phase and the solvent-vapor phase, and that they can be related by a modified Raoult's Law:

$$P_s = x_s \gamma_s P_s^{\text{sat}}, \tag{7}$$

where P_s is the partial pressure of the solvent vapor and P_s^{sat} is the saturated vapor pressure of the solvent. Combining Eqs. (3), (6), and (7) leads to an implicit relationship for t_{solv}

$$\ln\left(\frac{t_{\text{solv}} - t_{\text{dry}}}{t_{\text{solv}}}\right) + \left(\frac{t_{\text{dry}}}{t_{\text{solv}}}\right) + \chi\left(\frac{t_{\text{dry}}}{t_{\text{solv}}}\right)^2 = \ln\left(\frac{P_s}{P_s^{\text{sat}}}\right). \tag{8}$$

In obtaining Eq. (8), we make use of the fact that $m \gg 1$, so that $m^{-1} \cong 0$. Although in this expression the polymer thickness appears to depend only on χ and the solvent-vapor partial pressure P_s, there is an implicit dependence on temperature through P_s^{sat}. P_s^{sat} can be expressed by the Antoine vapor-pressure correlation:

$$P_s^{\text{sat}} = \exp\left[AntA - \frac{AntB}{T + AntC} \right] \text{ torr}, \tag{9}$$

where for acetone $AntA = 16.65$, $AntB = 2940.46$ K, and $AntC = -25.93$ K.[23]

In general, the polymer-solvent interaction parameter χ can depend on both temperature and composition (ϕ_p, ϕ_s) for a given system. However, since the composition dependence is often weak and only a modest range of temperatures (~ 35 °C) is employed in our experiments, we determined a single average value of $\chi = 1.53$ by adjusting it to fit Eq. (8) to data at different temperatures and pressures. A higher value of χ corresponds to a weaker polymer-solvent interaction, and for a polymer with a high-molecular-weight $\chi > 0.5$ indicates the existence of an immiscibility gap over some composition (ϕ_p, ϕ_s) where a homogeneous solution is not formed.[21] Indeed, acetone will not dissolve the PVK/PBD film, as expected for a value of $\chi = 1.53$. The dependence of polymer swelling on χ is made apparent by taking the exponential of Eq. (8) and expanding the left side for small $t_{\text{solv}} - t_{\text{dry}}$. To first order in thickness increase $t_{\text{solv}} - t_{\text{dry}}$ (corresponding to small solvent content $\phi_s \ll 1$), we find

$$\frac{t_{\text{solv}} - t_{\text{dry}}}{t_{\text{dry}}} \cong e^{-(1+\chi)} \frac{P_s}{P_s^{\text{sat}}}. \tag{10}$$

This more intuitive relationship indicates that for small polymer swelling, the fractional increase in thickness $(t_{\text{solv}} - t_{\text{dry}})/t_{\text{dry}}$ is linear with solvent-vapor pressure and depends exponentially on χ. A low χ corresponds to strong solvent-polymer interactions, leading to greater swelling. As noted before, the temperature dependence enters through P_s^{sat}, which increases with temperature according to Eq. (9).

Figures 7(a) and 7(b) compare the model [Eq. (6), with $\chi = 1.53$] to the experimentally determined film thickness increases at different acetone partial pressures and sample temperatures. The model, which has only a single fitting parameter χ, matches the experimental measurements reasonably well, reproducing the linear dependence of thickness on vapor pressure at low vapor pressures. The dependence on temperature is also well modeled. The predicted thickness increase with vapor pressure is very large at high vapor pressures and low temperatures. This may partially explain the difficulties in reproducing the data in this range, as noted in the previous section.

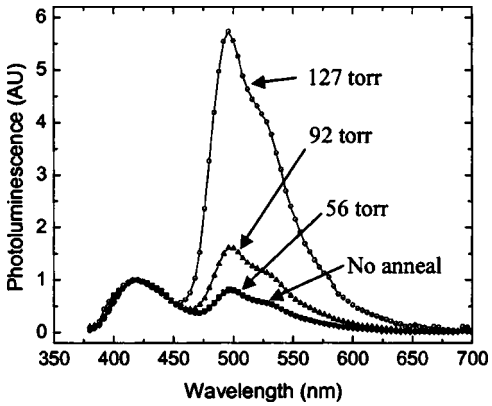

FIG. 10. Photoluminescence spectra of PVK/PBD/C47 samples with a printed layer of C6 dye after 10-min acetone-vapor anneals at different partial pressures at 18 °C. Also shown is an as-printed spectrum, which is indistinguishable from the 56-torr spectrum. All spectra have been normalized to the C47 emission peak at 420 nm.

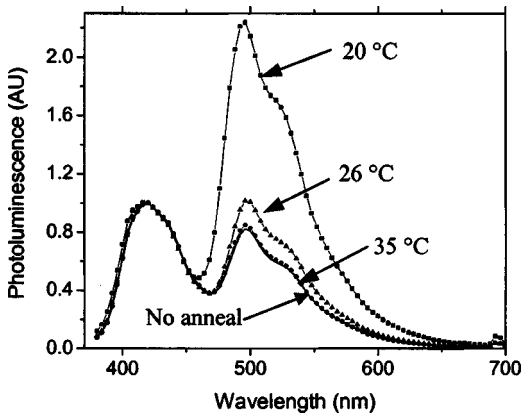

FIG. 11. Photoluminescence spectra of PVK/PBD/C47 films (illuminated through the sapphire substrate) that have been annealed in acetone vapor (120 torr) for 10 min at different sample temperatures after dye printing. Also shown is an as-printed spectrum, which is indistinguishable from the 35 °C spectrum. All spectra have been normalized to the C47 emission peak.

IV. DYE DIFFUSION

A. Dye-diffusion experiments

The absorption of solvent vapor by a polymer film results in a thicker film with greater free volume in which the diffusion of dye molecules is greatly enhanced. In this section, we present experimental results for dye diffusion in solvent-swollen polymers.

Dye source plates containing the dye C6 were prepared as described in Sec. II A. The dye source plate was not patterned in these experiments, although extensive experiments have been done with patterned plates to make multiple regions of different emitting colors on a single substrate. The details of these experiments are reported elsewhere.[24]

The SIMS measurements presented earlier (Fig. 2) showed that far more diffusion occurred at room temperature in acetone vapor (90 torr) than at 92 °C without solvent. Straightforward modeling of these curves shows that at room temperature with acetone vapor, the C6 diffusion coefficient was $>10^{-13}$ cm^2/s, whereas it was $\sim 10^{-17}$ cm^2/s without solvent vapor at 92 °C.

To observe the optical activity of the dye as a function of depth, a solution of PVK/PBD mixed with the dye coumarin-47 (C47, emission peak at 420 nm, 0.2% by weight) was spun onto an UV-transparent sapphire substrate, resulting in a film with C47 (a blue-emitting dye) distributed uniformly throughout the depth of the film. After C6 printing and solvent exposure, the PVK/PBD/C47 films were exposed to UV (254 nm) light either directly or through the sapphire substrate. The resulting PL spectrum was recorded from the side that was illuminated. Each spectrum was normalized to the peak of the C47 signal. The absorption length in PVK/PBD at this wavelength is only 50 nm,[17] so the height of the C6 emission peak (relative to the C47 peak) measures the quantity of C6 present in the top portion of the film (for direct UV exposure) or in the bottom portion (for exposure through the substrate).

The PL spectra of PVK/PBD/C47 samples (with a printed C6 layer) before and after acetone anneals at various partial pressures are shown in Fig. 10. Each sample was held at 18 °C during the 10-min acetone-vapor exposure and then illuminated from the front by an UV source to obtain the PL spectra. Initially, the C6 emission is minimal, which indicates that the C6 is primarily on the polymer surface, making it inactive. Annealing at a low partial pressure (56 torr), corresponding to a polymer thickness increase of ~3%, is not sufficient to increase the C6 emission. As the partial pressure is raised to 92 torr (~5% thickness increase) or 127 torr (~9% increase), the C6 is able to diffuse into the polymer and the C6 emission peak is enhanced dramatically.

Similar results are obtained when the sample temperature is varied and the acetone partial pressure (120 torr) is kept constant (Fig. 11). In this measurement, PL spectra were obtained by illuminating the sample through the UV-transparent substrate. Each spectrum is therefore dominated by dye present in the bottom of the film. As in the PL from the top surface in Fig. 10, the anneal at 35 °C (~3% thickness increase) is not sufficient to diffuse dye into the film and increase the magnitude of the C6 peak relative to the as-printed value. However, lower temperatures of 26 °C and 20 °C, corresponding to 6% and 10% thickness increases, result in enhanced dye diffusion to the bottom of the film, as reflected by the increase of the C6 peak. These data confirm that solvent vapor can greatly increase the dye diffusion and, most surprisingly, that in the presence of a solvent vapor more diffusion occurs as the temperature is lowered.

SIMS measurements on similarly treated samples were used to confirm this trend. Figure 12 plots sulfur (C6) profiles in 90-nm PVK/PBD samples as-printed and after 2 -min anneal at 35 °C and 19 °C (acetone partial pressure =120 torr). It is evident that the 35 °C (~4% thickness increase) anneal leads to minimal dye diffusion into the film, whereas the 19 °C anneal (~10% thickness increase) leads to a uniform dye distribution throughout the layer in only a few minutes. We note that other workers, who also employed a dye-diffusion process in solvent vapor, observed a more conventional trend of increased diffusion at elevated temperatures.[4] In their work, the dye source and target films were exposed to solvent vapor and then placed in contact and

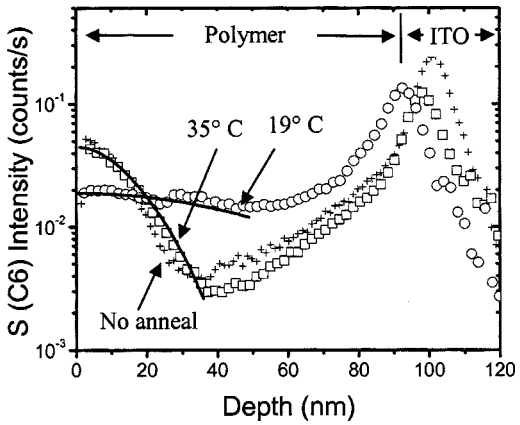

FIG. 12. SIMS analysis of PVK/PBD films following printing of C6 dye and 2-min acetone vapor (120 torr) anneals at 19 °C and 35 °C. The sulfur-signal rise in two samples starting at a depth of 50 nm is thought to be O_2 from the substrate. Also shown are fits to the 19 °C and 35 °C anneals derived from numerical modeling of the C6 diffusion (solid lines); the fits correspond to the diffusion coefficients of 5×10^{-13} cm^2/s and 3×10^{-15} cm^2/s, respectively.

heated (using relatively high temperatures of 80–200 °C) to transfer and diffuse the dye while maintaining the solvent-vapor atmosphere. The contact between the dye and source plates may have limited solvent evaporation at elevated temperatures, leading to a trend opposite to that observed in our work.

Dye diffusion coefficients were estimated from the SIMS data by numerical modeling. Constant diffusion from a finite plane source was assumed.[25] Fits to the 19 °C and 35 °C anneals in solvent vapor are shown in Fig. 12. Due to the uncertainty in the as-printed and annealed profiles caused by the "knock-on" effects during the SIMS measurement discussed in Sec. II, the absolute error in diffusion coefficients could be as large as a factor of 5. The diffusion coefficients are plotted in Fig. 13, along with diffusion coefficients from thermally annealed samples.[13] The enhancement of diffusion by acetone vapor is enormous. If the thermal diffusion coefficients from 90–130 °C are extrapolated to 20 °C, we would expect a diffusion coefficient of $\sim10^{-30}$ cm^2/s, which is nearly 10^{18} times less than the solvent-enhanced diffusion at the same temperature. Furthermore, in the presence of the solvent vapor, the dye diffusion decreases as the temperature is increased, a most peculiar circumstance. This occurs because the solvent effect is so pronounced. At higher temperatures, the film absorbs less solvent, as discussed in Sec. III. The resulting decrease in solvent-enhanced diffusion at higher temperatures more than offsets the relatively smaller increase in conventional thermal diffusion.

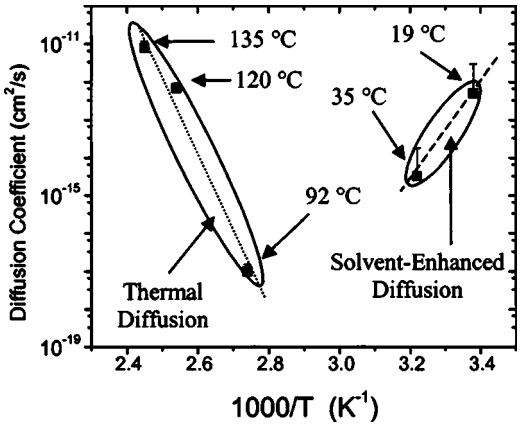

FIG. 13. Diffusion coefficients of C6 in PVK/PBD vs inverse temperature for thermal diffusion and solvent-enhanced diffusion (acetone vapor, 120 torr).

B. Dye-diffusion discussion

The diffusion of small molecules in polymers is generally characterized by two regimes. At low temperatures, the polymer film is in a glassy state with very limited diffusion. As the polymer is heated above a certain temperature (T_g), it enters a rubbery state and diffusion is rapidly increased. Conceptually, the diffusion of molecules into a polymer film requires the existence of voids into which the molecules can move. Above T_g, polymer relaxation processes are relatively quick, leading to the ready formation of voids and rapid diffusion of small molecules.[26] Below T_g, these relaxation processes require long time scales, which limits the amount of free volume available for diffusion. The PVK/PBD blend (100:40 by weight) (with no solvent present) has been measured to have a T_g=120 °C.[16] This indicates that process temperatures greater than 120 °C are desirable to diffuse dye into this blend; however, these temperatures are sufficient to cause significant degradation of the PVK. Lowering T_g is therefore preferable to raising T.

The introduction of acetone into the PVK/PBD blend has the effect of lowering the effective glass transition temperature $T_{g,eff}$ of the film. It is well known that T_g of a polymer can be changed by mixing it with a material having a different T_g. The Fox equation[27] can be used to estimate $T_{g,eff}$ of a blend with components having mass fractions w_i and glass transition temperatures T_{gi}:

$$\frac{1}{T_{g,eff}} = \sum_i \frac{w_i}{T_{gi}}. \tag{11}$$

A common approximation is to estimate T_g of a solvent as two-thirds of its melting temperature.[28] For acetone, the melting temperature is 178 K, so that $T_g \sim 120$ K. $T_{g,eff}$ of the solvent-swollen polymer blend can be estimated by assuming that the measured thickness increase is equal to the volume of acetone present in the film (as was confirmed by modeling the change in index of refraction in Sec. III B). For example, an increase of thickness of 10% in acetone vapor implies an acetone volume fraction of 0.1/1.1=0.09 and a PVK/PBD volume fraction of 1/1.1=0.91. The densities of acetone ($\sim$0.8 g/cm^3) and PVK and PBD (both $\sim$1.2 g/cm^3) are used to convert these volume fractions into weight fractions; we can then use Eq. (11) to find a decrease in T_g of the PVK/PBD blend of 50 °C.

We call the glass transition temperature of the mixture (polymer and solvent) an effective glass transition temperature $T_{g,eff}$. This is because it is not actually possible to raise the temperature of the mixture in practice to reach this lowered $T_{g,eff}$ because as the temperature is raised the solvent uptake decreases, thus increasing $T_{g,eff}$. Defining a lower $T_{g,eff}$ for the films is still a useful concept, however, because

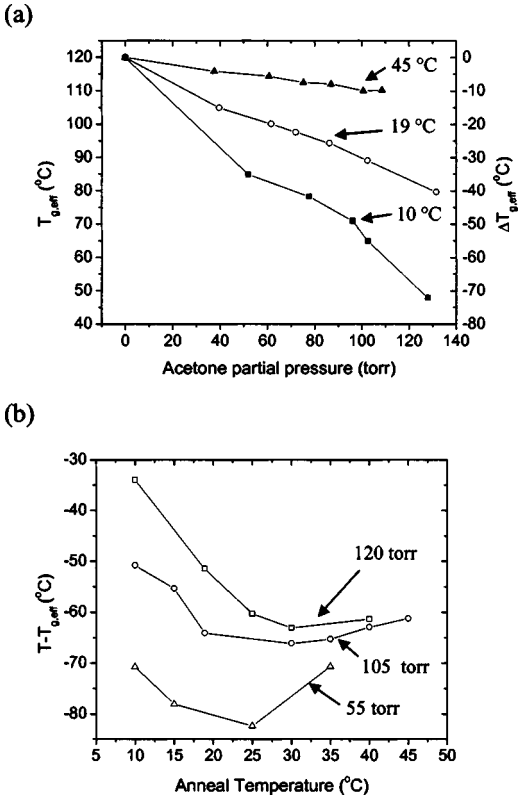

FIG. 14. (a) Calculated effective glass transition temperature $T_{g,eff}$ of the PVK/PBD film (based on measured thickness increase) as a function of acetone partial pressure for various annealing temperatures. (b) T-$T_{g,eff}$ as a function of T for various acetone partial pressures.

$T_{g,eff}$ represents the increased free volume which enables dye diffusion, so that $(T-T_{g,eff})$ should correlate with the enhanced diffusion.

Figure 14(a) shows $T_{g,eff}$ calculated from Eq. (11) as a function of vapor pressure for temperatures of 10 °C, 19 °C, and 45 °C (using data from Fig. 7). Although the decrease in $T_{g,eff}$ is minimal at 45 °C, at a lower temperature of 19 °C, $T_{g,eff}$ can be reduced from 40° to 80 °C, whereas at a temperature of 10 °C, it can be reduced by up to 70° to lower $T_{g,eff}$ to 50 °C.

In Fig. 14(b), the difference between the process temperature and the effective glass transition temperature $(T-T_{g,eff})$ is plotted as a function of temperature for different acetone-vapor pressures. In all cases, T_g remains well above the process temperatures (implying that the polymer remains in a glassy state) yet still we know experimentally that extensive diffusion can occur. For quantitative modeling of D, a diffusion model that is valid for $T<T_{g,eff}$ would be necessary. Although several models for diffusion above and around T_g have been proposed,[29–34] diffusion in glassy polymers is complicated and difficult to model quantitatively.[35] Nevertheless, it is clear that reducing $T_{g,eff}$ of the polymer film to approach the process temperature leads to dramatically enhanced diffusion. This dependence of dye diffusion on $(T-T_{g,eff})$ is illustrated by the trends depicted in Fig. 14(b). Here, $(T-T_{g,eff})$ is the highest at a low sample temperature, where the decrease in $T_{g,eff}$ due to enhanced absorption of solvent vapor more than offsets the relatively low temperature. $(T-T_{g,eff})$ actually decreases as T is raised to ~35 °C due to evaporation of the solvent, and then begins to increase slightly as negligible amounts of solvent absorption occur and the system enters a normal, thermally activated diffusion regime. This plot correctly explains the observed dye-diffusion trend, which in contrast to conventional diffusion is highest at low temperatures, where $(T-T_{g,eff})$ is largest.

V. SUMMARY

Through exposure to solvent vapor, the diffusion of printed dye on a polymer surface through the film can be completed at room temperature. Thus, thermal damage to the active polymer can be avoided while still employing a polymer layer with a high T_g for device stability. The enhancement of dye diffusion in acetone vapor is dependent on the amount of solvent vapor absorbed by the polymer, which causes it to increase its thickness. This thickness increase is largest at low temperatures and high solvent-vapor pressures and can be modeled based on Flory-Huggins theory. The absorbed solvent increases the dye-diffusion coefficient by many orders of magnitude. At high acetone partial pressures and/or low sample temperatures, diffusion times of only a few minutes were necessary to diffuse C6 dye throughout a 100-nm polymer layer. This enhancement is attributed to the reduction of $T_{g,eff}$ of the PVK/PBD blend as it absorbs acetone vapor, although it appears that lowering $T_{g,eff}$ to the process temperature (near room temperature) was not necessary.

ACKNOWLEDGMENTS

This work was supported by NJCST and DARPA. One of the authors (T.G.A.) was supported by NDSEG.

[1] G. Parthasarathy, J. Liu, and A. R. Duggal, Electrochem. Soc. Interface **12**, 42 (2003).
[2] F. Pschenitzka and J. C. Sturm, Appl. Phys. Lett. **74**, 1913 (1999).
[3] A. Nakamura, T. Tada, M. Mizukami, S. Hirose, and S. Yagyu, Appl. Phys. Lett. **80**, 2189 (2002).
[4] C.-C. Wu, S.-W. Lin, C.-W. Chen, and J.-H. Hsu, Appl. Phys. Lett. **80**, 1117 (2002).
[5] K. Tada and M. Onoda, Jpn. J. Appl. Phys., Part 2 **38**, L1143 (1999).
[6] S.-C. Chang, J. Bhanathan, and Y. Yang, Appl. Phys. Lett. **73**, 2561 (1998).
[7] J. Bharathan and Y. Yang, Appl. Phys. Lett. **72**, 2660 (1998).
[8] T. R. Hebner, C. C. Wu, D. Marcy, M. H. Lu, and J. C. Sturm, Appl. Phys. Lett. **72**, 519 (1998).
[9] C. F. Madigan, T. R. Hebner, J. C. Sturm, R. A. Register, and S. Troian, Mater. Res. Soc. Symp. Proc. **624**, V.3.5 (2000).
[10] F. Pschenitzka and J. C. Sturm, Appl. Phys. Lett. **78**, 2584 (2001).
[11] K. Long, F. Pschenitzka, and J. C. Sturm (unpublished).
[12] J. Kido, S. Shirai, Y. Yamagata, and G. Harada, presented at the Materials Research Society Spring Meeting, San Francisco 1998 (unpublished).
[13] F. Pschenitzka and J. C. Sturm, Proc. SPIE **4105**, 59 (2001).
[14] C. C. Wu, J. C. Sturm, R. A. Register, J. Tian, E. P. Dona, and M. E. Thompson, IEEE Trans. Electron Devices **44**, 1269 (1997).
[15] F. Pschenitzka, K. Long, J. C. Sturm, Mater. Res. Soc. Symp. Proc. **665**, C9.5.1 (2001).
[16] X. Jiang and R. A. Register (private communication).
[17] J. M. Pearson and M. Stolka, *Poly(N-vinyl carbazole)* (Gordon and Breach, New York, 1981).
[18] O. Heavens, *Optical Properties of Thin Solid Films* (Dover Publications, New York, 1965).
[19] *Polymer Handbook*, 3rd ed. edited by J. Brandrup and E. H. Immergut (Wiley, New York, 1989).
[20] P. Brocos, A. Pineiro, R. Bravo, and A. Amigo, Phys. Chem. Chem. Phys.

5, 550 (2003).
[21]P. Flory, *Principles of Polymer Chemistry* (Cornell University Press, Ithaca, NY, 1953).
[22]J. M. Smith and H. C. Van Ness, *Introduction to Chemical Engineering Thermodynamics*, 4th ed. (McGraw-Hill, New York, 1987).
[23]R. Reid, J. M. Prausnitz, and T. K. Sherwood, *The Properties of Gases and Liquids*, 3rd ed. (McGraw-Hill, New York, 1987).
[24]K. Long, F. Pschenitzka, and J. C. Sturm, Mater. Res. Soc. Symp. Proc. **708**, BB6.8 (2001).
[25]The assumption of a constant diffusion coefficient implies that there is a stable, uniform concentration of acetone already present in the film. Measurements of the time dependence of the PVK/PBD thickness increase upon exposure to acetone vapor (Sec. III) indicate that the acetone does indeed diffuse rapidly throughout the film (on time scales of less than 1 s). However, in the large-volume chamber used in the diffusion experiments, a larger thickness-increase time constant of 79 s was measured due to the longer time necessary for the acetone vapor to reach equilibrium pressure. The assumption of constant diffusion is therefore not entirely justified. This leads to some additional error in the estimate of the dye-diffusion coefficient, but the predominant source of error is uncertainty in the initial and final dye profiles.
[26]T. E. Shearmur, D. W. Drew, A. S. Clough, M. G. D. Van der Grinten, and A. T. Slark, Polymer **37**, 2695 (1996).
[27]T. G. Fox, Bull. Am. Phys. Soc. **1**, 123 (1956).
[28]D. W. V. Krevelen, *Properties of Polymers: Their Correlation with Chemical Structure, Their Numerical Estimation, and Prediction from Additive Group Contributions*, 3rd ed. (Elsevier, Amsterdam, 1990).
[29]M. L. Williams, R. F. Landel, and J. D. Ferry, J. Am. Chem. Soc. **77**, 3701 (1955).
[30]M. H. Cohen and D. J. Turnbull, J. Chem. Phys. **31**, 1164 (1959).
[31]H. Fujita, Fortschr. Hochpolym.-Forsch. **3**, 1 (1961).
[32]J. S. Vrentas and J. L. Duda, J. Polym. Sci., Polym. Phys. Ed. **15**, 403 (1977).
[33]D. Ehlich and H. Sillescu, Macromolecules **23**, 1600 (1990).
[34]J. S. Kim and K. R. Lee, Polymer **41**, 8441 (2000).
[35]A.-C. Dubreuil, F. Doumenc, B. Guerrier, and C. Allain, Macromolecules **36**, 5157 (2003).